The Astrophysical Journal, 514:L121–L124, 1999 April 1

DETECTION OF THE CN ZEEMAN EFFECT IN MOLECULAR CLOUDS

Richard M. Crutcher,[1] Thomas H. Troland,[2] Bernard Lazareff,[3] Gabriel Paubert,[4] and Ilya Kazès[5]
Received 1998 December 9; accepted 1999 January 27; published 1999 February 9

ABSTRACT

Observations of the Zeeman effect in the 3 mm lines of CN have been carried out with the 30 m IRAM telescope toward seven dense molecular clouds. Detections were achieved toward the Orion Molecular Cloud 1 (OMC1), toward two cores in the DR21OH molecular cloud, and probably toward the M17SW molecular cloud. The line-of-sight magnetic field strengths inferred are $B_{\rm los}$(OMC1) = −0.36 ± 0.08, $B_{\rm los}$(DR21OH$_1$) = −0.36 ± 0.10, $B_{\rm los}$(DR21OH$_2$) = −0.71 ± 0.12, and $B_{\rm los}$(M17SW) = −0.33 ± 0.14 mG. The theoretical implications of these results are discussed.

Subject headings: ISM: clouds — ISM: magnetic fields — stars: formation

1. INTRODUCTION

Understanding the physics governing the structure and evolution of dense interstellar clouds is a necessary part of understanding the fundamental astrophysical process of star formation. In the past decade, it has become increasingly clear that this physics cannot be understood in the absence of magnetic fields. Theoretical work on the evolution of the interstellar medium, the formation and evolution of clouds, and the formation of stars is a very active area of current research. In order to provide an empirical basis for the theory, it is essential to vigorously pursue observations of magnetic field morphologies and strengths.

The only currently viable technique for measuring the strengths of magnetic fields in interstellar clouds is to detect the Zeeman effect in spectral lines arising in the clouds. Zeeman-effect measurements have been made in thermally excited lines of H I and OH. However, dense clouds are molecular with very little H I, and the OH radical is highly reactive and decreases in relative abundance at high densities. Although observations of OH and H_2O masers probe high densities, masers arise in very small regions under special conditions and do not allow measurements of magnetic fields in distributed but high-density clouds. Zeeman-effect measurements that are sensitive to magnetic fields in extended high-density regions are essential.

Several years ago, we began an effort to probe magnetic fields in dense clouds by attempting to detect the Zeeman effect in the 3 mm lines of CN (Crutcher et al. 1996). We have continued those efforts and here report further results, which include the first detections of the CN Zeeman effect.

2. OBSERVATIONS

Crutcher et al. (1996) discussed the physics of the CN Zeeman effect and argued that CN offers the best opportunity to measure magnetic fields in clouds with densities of 10^5–10^6 cm^{-3}. The CN ground state is $^2\Sigma$, and the $N = 1$–0 transition at $\nu \approx 113.5$ GHz has a total of nine hyperfine components, of which seven have relatively strong intensities (Table 1 of Crutcher et al. 1996). Of these, four have a strong Zeeman effect. The fact that different components have very different Zeeman splitting coefficients makes it possible to derive the Zeeman effect and instrumental effects separately in the form of three independent possible contributions to a Stokes V spectrum: (1) the Zeeman splitting, (2) beam squint, which (together with a velocity gradient in the molecular cloud) could produce a pseudo-Zeeman splitting, and (3) the polarization leakage between right- and left-circularly polarized receiver channels. The procedure is to fit simultaneously over the seven hyperfine components for the three coefficients a, b, and c in the equation $V = aI + bZ(dI/d\nu) + c(dI/d\nu)$, where V is the Stokes V spectrum, I is the Stokes I spectrum, and Z is the Zeeman splitting coefficient for each of the seven hyperfine components. Details of our fitting procedure are described in Crutcher et al. (1996).

All observations were carried out with the 30 m IRAM telescope, which has a full width at half-power (FWHP) beam diameter of 23″ at 113 GHz. The typical system temperature was about 300 K. Our first observations were obtained during a 1994 session; the negative results toward OMC1-N4 and S106 have been reported previously (Crutcher et al. 1996). Subsequently, we had three additional observing sessions, in 1995, 1996, and 1997. During the 1995 session, the identical polarimeter and single 3 mm receiver described in Crutcher et al. (1996) were used. After the 1995 session, IRAM added a second 3 mm receiver, which made it possible to observe simultaneously right- and left-circular polarization rather than time multiplexing polarizations. Switching polarizations between receiver channels every few seconds was still employed in order to reduce possible systematic effects. Use of both receivers required the construction of a new polarimeter with a larger quarter-wave polarization plate. Although useful data were obtained with this system in 1996, a better quarter-wave plate was constructed and used for the 1997 observations. Except for observing both polarizations simultaneously for some of the observations, all observing and data processing procedures were unchanged from those of the 1994 observing session (Crutcher et al. 1996).

In the 1995 session, we attempted to observe a number of molecular clouds for relatively brief times in order to identify a small number for deep integrations. The most promising molecular clouds for detection of the Zeeman effect in CN were those toward OMC1n, DR21OH, and M17SW. The 1996 and 1997 sessions concentrated on positions in those three clouds;

[1] Astronomy Department, University of Illinois, Urbana, IL 61801.
[2] Physics and Astronomy Department, University of Kentucky, Lexington, KY 40506.
[3] Institut de Radioastronomie Millimétrique, 300, Rue de la Piscine, Domaine Universitaire, 38406 Saint-Martin-D'Hères, France.
[4] Instituto de Radioastronomia Milimetrica, Avenida Divina Pastora, 7, Núcleo Central, E-18012 Granada, Spain.
[5] Observatoire de Paris-Section de Meudon, Place Jules Janssen, F-92195 Meudon, France.

TABLE 1
CLOUDS OBSERVED AND RESULTS FROM GLOBAL ZEEMAN FITS

Cloud	α(1950)	δ(1950)	V_{LSR} (km s^{-1})	T_A (K)	ΔV (km s^{-1})	τ (hr)	B_{los} (mG)
OMC1n	05 32 47.0	−05 24 00	+10	14	1.9	50.3	−0.19 ± 0.09
OMC1s	05 32 46.0	−05 24 45	+10	15	2	6.8	+ 0.04 ± 0.24
OrionB	05 39 13.5	−01 57 15	+10	9	2.4	3.8	+ 0.27 ± 0.33
M17SWn	18 17 29.8	−16 12 55	+20	17	3.2	3.6	−0.33 ± 0.14
M17SWs	18 17 31.8	−16 15 05	+20	17	2.0	10.0	−0.22 ± 0.22
DR21OH	20 37 13.0	+42 12 00	−3	5	2 × 2.3	48.0	−0.45 ± 0.15
S140	22 17 40.0	+63 03 30	−7	6	2.6	6.3	−0.27 ± 0.40

NOTE.—Units of right ascension are hours, minutes, and seconds, and units of declination are degrees, arcminutes, and arcseconds.

unfortunately, weather conditions and its low declination prevented significant additions to our integration times on M17SW.

3. RESULTS

The positions, line velocities, antenna temperatures of the strongest hyperfine component ($[N', J', F'] \rightarrow [N, J, F] = [1, 3/2, 5/2] \rightarrow [0, 1/2, 3/2]$), FWHP line widths, single-receiver equivalent integration times, and line-of-sight magnetic field strengths and 1 σ errors are listed in Table 1 for the seven clouds with significant integration times. To derive these results, we obtained $dI/d\nu$ by numerically differentiating the observed Stokes I spectra. Since our simultaneous fitting process solves separately for possible instrumental effects and for a real Zeeman splitting, we believe that spurious signals are unlikely and that results at the 2 σ level are likely to be real. Hence, the results for OMC1n, M17SWn, and DR21OH are probably detections of the CN Zeeman effect.

In examining the spectra obtained during the deeper integrations toward the OMC1n and the DR21OH positions, we found that there were two velocity components toward each position. The Zeeman signals seen in the Stokes V spectra suggested that a different magnetic field was present in each velocity component. We therefore fitted two Gaussians to each of the seven Stokes I hyperfine components for each of the two clouds, imposing the constraint that the line widths and velocities be the same for the seven hyperfine components. We then derived $dI/d\nu$ by differentiation of the Gaussians. This procedure allowed us to infer the magnetic field separately in each velocity component and had the additional advantage that no noise was introduced into the fitting process by channel-to-channel noise in $dI/d\nu$. The fits to the observed Stokes V spectra therefore had five parameters: the polarization leakage a, the Zeeman effects b_1 and b_2 for the two velocity components, and the pseudo-Zeeman signals c_1 and c_2 produced by velocity gradients for the two velocity components. For OMC1n, one of the velocity components had $V_{LSR} = -9.23$ km s^{-1} and $\Delta V = 3.7$ km s^{-1} (ΔV is the FWHP of the line). This broad line component had no Zeeman effect and is not considered further. Results for each of the other velocity components are listed in Table 2.

TABLE 2
RESULTS FROM VELOCITY-COMPONENT FITS

Item	DR21OH$_1$	DR21OH$_2$	OMC1n$_1$
V_{LSR} (km s^{-1})	−4.66	−0.93	+9.94
ΔV (km s^{-1})	2.3	2.3	1.4
B_{los} (mG)	−0.36 ± 0.10	−0.71 ± 0.12	−0.36 ± 0.08
n (H$_2$ cm^{-3})	1 × 10^6	2 × 10^6	8 × 10^5
N (H$_2$ cm^{-2})	2 × 10^{23}	4 × 10^{23}	2 × 10^{23}
T_K (K)	50	50	100
Radius (pc)	0.05	0.05	0.05
Mass ($M_\odot$)	35	70	30
m_s	4.0	4.0	1.7
m_A	1.8	1.3	1.0
β_p	0.41	0.21	0.65
$\mathcal{T}/\mathcal{W}$	0.6	0.3	0.3
$\mathcal{M}/\mathcal{W}$	0.09	0.09	0.14
$[M/\Phi_B]_{obs/crit}$	2.8	2.8	2.2

The derivation of the Zeeman signal comes from a simultaneous fit to all seven hyperfine components and includes fits for instrumental effects. It is therefore not straightforward to see the Zeeman signal in plots of the Stokes V spectra of the seven hyperfine components. In order to illustrate the data for OMC1n and DR21OH, we have produced separate weighted average spectra for the four hyperfine components that have the strongest Zeeman splitting coefficients and the three that have negligible Zeeman splitting. The four Zeeman-sensitive hyperfine components are lines 1, 4, 5, and 7 in Table 1 of Crutcher et al. (1996). The weighting of the four Zeeman components is by the relative sensitivity to the Zeeman effect—the Zeeman-splitting coefficient Z times the relative intensity for each hyperfine component. The weighting of the three components with small Zeeman-splitting coefficients is by the relative intensity for each hyperfine component. The weighted-average spectra are shown in Figures 1 and 2. The top panels show the weighted-average Stokes $I/2 = (L + R)/2$ spectrum for the four Zeeman-sensitive components; the Stokes I spectrum for the other three components is similar except for a different intensity. The middle panels show the observed $V = L - R$ spectrum for the four Zeeman-sensitive components corrected for the instrumental effects; that is, $V_{observed} - a(I_1 + I_2) - c_1(dI_1/d\nu) - c_2(dI_2/d\nu)$. Hence, the only signal remaining in the observed V spectrum should be the Zeeman signal, $b_1\bar{Z}(dI_1/d\nu) + b_2\bar{Z}(dI_2/d\nu)$. The fit to this observed, corrected V spectrum is also shown. The bottom panels show the observed and fitted V spectra for the three hyperfine components with low Zeeman sensitivity (lines 2, 3, and 6). The ratio of the sensitivity to the Zeeman effect for the two sets of components is $\bar{Z} \times \bar{I} = 5.8$. The fact that the Zeeman-sensitive hyperfine components show a Stokes V signal and the three components that are not Zeeman sensitive do not is strong evidence that the Zeeman effect has been detected.

4. DISCUSSION

The magnetic field toward M17 has been mapped with the H I Zeeman effect in absorption with the VLA by Brogan et al. (1999). They argue that the H I velocity component at 20 km s^{-1} samples gas in the photodissociation region between the shock and the I-front at the interface between the H II region and the M17SW molecular cloud and that their B_{los} map is actually a map of the magnetic field in dense molecular gas.

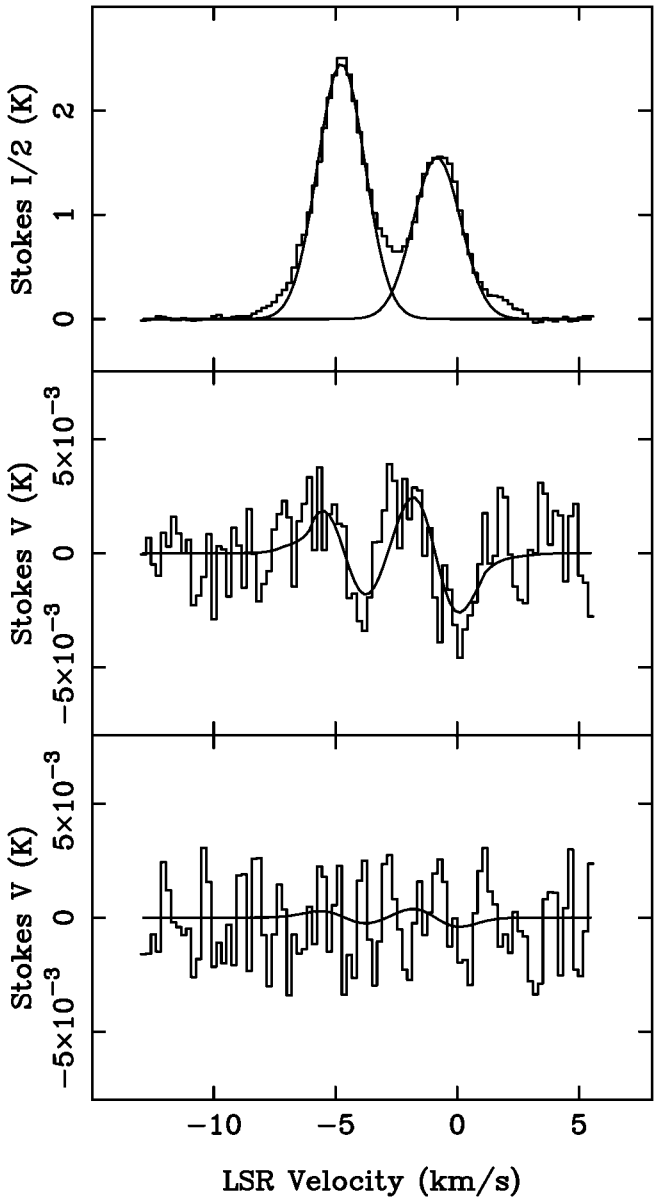

FIG. 1.—Averaged CN spectra for DR21OH. *Top and middle:* Averaged $I/2$ and V spectra for the four Zeeman-sensitive hyperfine components. *Bottom:* Averaged V spectrum for the three hyperfine components with weak Zeeman sensitivity. The histogram plots show the data; the lines show the Gaussians fitted to the I spectrum and $dI/d\nu$ fitted to the V spectra.

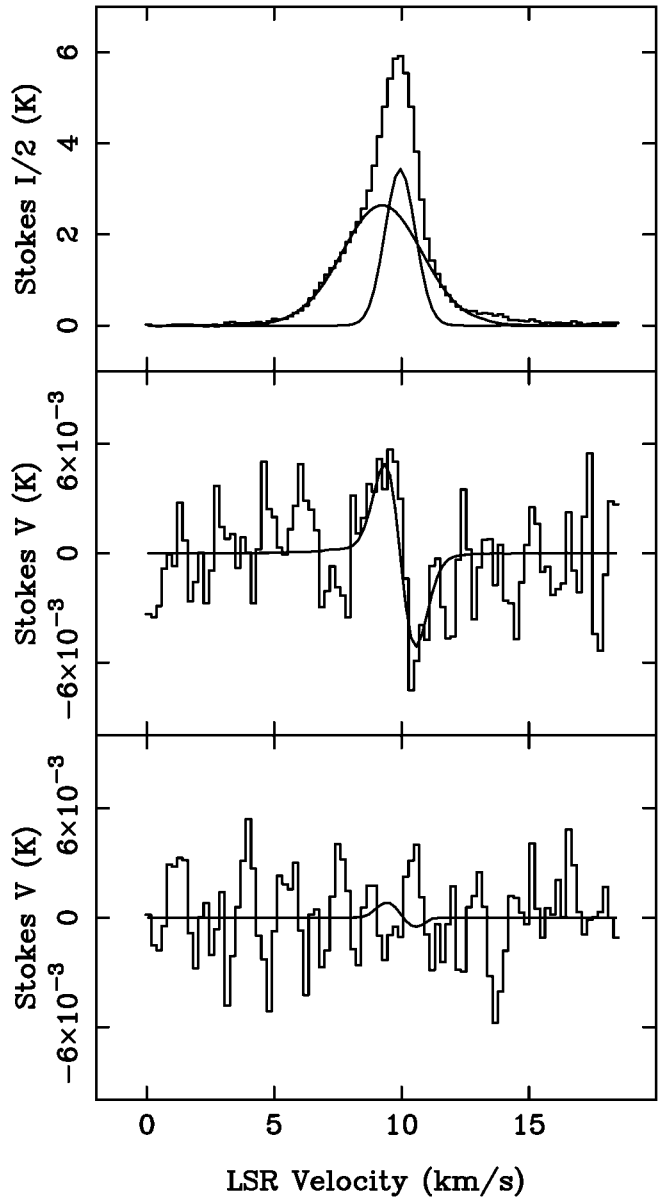

FIG. 2.—As in Fig. 1, but for OMC1n

Their peak B_{los} is approximately equal to -0.45 mG at the H II/H_2 interface, with $B_{los} \approx -0.1$ mG at positions toward the H II region and away from the molecular cloud. Our M17 positions are at peaks in the M17SW molecular cloud near the interface with the H II region. The CN positions are just north and south of where the VLA map shows the B_{los} measured in H I, but the VLA map shows that $B_{los} \approx -0.2$ mG in the region between the CN positions. Hence, the VLA H I and our CN measurements are consistent and suggest that $B_{los} \approx -0.2$ to -0.4 mG in the M17SW molecular cloud. Brogan et al. (1999) extensively discuss the magnetic field in M17, and our CN data add little to their discussion except for providing a consistency argument for the interpretation that the H I samples the magnetic field in the molecular cloud.

The two velocity components toward DR21OH are almost cleanly separated in velocity. The velocities are $V_{LSR} \approx -4.66$ and -0.93 km s^{-1}; these are labeled DR21OH$_1$ and DR21OH$_2$, respectively. B_{los} was derived separately for the two components as described above. These components correspond to two cores within the single IRAM beam which were (marginally) resolved by Owens Valley Radio Observatory synthesis mapping of the $C^{18}O$ line (Padin et al. 1989); the $C^{18}O$ data were used to infer the physical parameters listed in Table 2.

Toward OMC1 the CN emission does not peak at the OMC1 hot core, but at two locations just north and south of the core. We observed both peaks; they are labeled OMC1n and OMC1s in Table 1. The CN detection was toward the OMC1n position, which is ≈24″ north of the IRc2 position. The study of Rodríguez-Franco et al. (1992) of the molecular structure near OMC1 identified a clump which corresponds to the CN position and velocity. They refer to this clump as the 10 km s^{-1} cloud. Physical parameters other than B_{los} were taken from their study.

These data may be used to compute standard parameters that

are important for assessing the importance of magnetic fields in star-forming clouds. These parameters are the following:

1. The sonic Mach number $m_s = \sqrt{3}\sigma/c_s$, where $\sigma = \Delta V/(8 \ln 2)^{1/2}$ is the observed one-dimensional velocity dispersion with ΔV the FWHP of a Gaussian, $c_s = (kT_K/\mu)^{1/2}$ is the isothermal sound speed, T_K is the kinetic temperature, and $\mu = 2.33 m_{\rm H}$ is the mean particle mass for a region of molecular hydrogen allowing for 10% helium.
2. The Alfvénic Mach number $m_{\rm A} = \sqrt{3}\sigma/V_{\rm A}$, where the Alfvén speed $V_{\rm A} = |\boldsymbol{B}|/(4\pi\rho)^{1/2}$, $|\boldsymbol{B}|$ is the strength of the magnetic field, and ρ is the gas density.
3. The ratio of thermal to magnetic pressures, $\beta_p = 2(m_{\rm A}/m_s)^2$.
4. The ratio of the mass to the magnetic flux $M/\Phi_B = 1.0 \times 10^{-20} N({\rm H}_2)/|\boldsymbol{B}|$ cm^2 μG [this is in units of the critical value $(M/\Phi_B)_{\rm crit} \approx 0.12/\sqrt{G}$; Mouschovias & Spitzer 1976; Nakano & Nakamura 1978].
5. The virial expressions for the gravitational energy $\mathcal{W} = (3/5)\, aGM^2/R$, the kinetic energy $\mathcal{T} = (3/2)\, M\sigma^2$, and the magnetic energy $\mathcal{M} = (1/3)\, b|\boldsymbol{B}|^2 R^3$, where we follow McKee et al. (1993) and take $a \approx 1.2$ and $b \approx 0.3$.

A significant problem is the fact that we measure only one component of $\boldsymbol{B}$. Statistically, for a random orientation of $\boldsymbol{B}$ with respect to the line of sight, the most probable values for $|\boldsymbol{B}|$ and $|\boldsymbol{B}|^2$ are $|\boldsymbol{B}| = 2B_{\rm los}$ and $|\boldsymbol{B}|^2 = 3B_{\rm los}^2$. We have therefore used twice the measured $B_{\rm los}$ in computing the parameters involving $|\boldsymbol{B}|$, namely m_A and M/Φ_B, and thrice the measured $B_{\rm los}^2$ in computing the parameters involving $|\boldsymbol{B}|^2$, namely β_p and $\mathcal{M}/\mathcal{W}$. Values of these parameters for the OMC1 and DR21OH clouds are listed in Table 2. Note, however, that these are only the most probable values, and for an individual cloud the correct values may differ substantially from the most probable values.

These results are too few and the uncertainties in physical parameters are too great to draw firm conclusions about the role of magnetic fields in dense cores. Considering these CN Zeeman results alone, however, we can say that while the motions in these three molecular cores are supersonic, they may be approximately Alfvénic ($m_{\rm A} \approx 1$), which suggests that MHD waves are responsible for the supersonic motions. The field strengths in these clouds, while large, are lower than might be expected if magnetic fields dominant the energetics. The parameter β_p is only slightly less than one, $\mathcal{T}$ appears to be significantly greater than $\mathcal{M}$, and $M/\Phi_B > 1$, so the clouds are magnetically supercritical. However, the cores are in approximate virial equilibrium ($2\mathcal{T} + \mathcal{M} \approx \mathcal{W}$), supported apparently primarily by internal motions rather than static magnetic fields. In such a case, processes that generate and dissipate mechanical energy would mainly control their future evolution. These CN Zeeman measurements form part of a growing set of measurements of magnetic field strengths that will eventually allow firm conclusions about the role of magnetic fields. Crutcher (1999) has discussed all of the available Zeeman measurements in molecular clouds (including the ones reported here) in order to carry out this type of analysis. Although the relative importance of magnetic fields seems to be somewhat reduced in the OMC1 and DR21OH cores compared with other (mainly lower density) clouds, the conclusions for these cores are in general agreement with those from the more comprehensive analysis of Crutcher (1999).

5. CONCLUSIONS

We have detected the Zeeman effect in the 3 mm lines of CN toward dense cores in the OMC1 and DR21OH molecular clouds and probably toward the M17SW molecular cloud, and we have inferred the line-of-sight magnetic fields from these data. The conclusions of this study are the following:

1. Gas velocities are supersonic but are approximately equal to the Alfvén velocity, which suggests that motions are due to MHD waves.
2. The ratios of thermal to magnetic pressures β_p are less than 1 (but only slightly).
3. The mass-to-magnetic flux ratios are supercritical by a factor of 2–3.
4. The clouds are in approximate virial equilibrium, with the kinetic energy apparently providing most of the support against gravity.

This research has been supported in part by the National Science Foundation under grants AST 94-19220 and AST 94-19227.

REFERENCES

Brogan, C. L., Troland, T. H., Roberts, D. A., & Crutcher, R. M. 1999, ApJ, in press
Crutcher, R. M. 1999, ApJ, in press
Crutcher, R. M., Troland, T. H., Lazareff, B., & Kazès, I. 1996, ApJ, 456, 217
Fiedler, R. A., & Mouschovias, T. Ch. 1993, ApJ, 415, 680
McKee, C. F., Zweibel, E. G., Goodman, A. A., & Heiles, C. 1993, in Protostars and Planets III, ed. E. H. Levy & J. I. Lunine (Tucson: Univ. Arizona Press), 327
Mouschovias, T. Ch., & Spitzer, L., Jr. 1976, ApJ, 210, 326
Nakano, T., & Nakamura, T. 1978, PASJ, 30, 671
Padin, S., et al. 1989, ApJ, 337, L45
Rodríguez-Franco, A., Martín-Pintado, J., Gómez-González, J., & Planesas, P. 1992, A&A, 264, 592